

Cross-Field Aerial Haptics: Rendering Haptic Feedback in Air with Light and Acoustic Fields

Yoichi Ochiai^{1*}, Kota Kumagai^{2*}, Takayuki Hoshi³, Satoshi Hasegawa² and Yoshio Hayasaki²

¹University of Tsukuba
Ibaraki, Japan
wizard@slis.tsukuba.ac.jp

²Utsunomiya University
Tochigi, Japan
{kumagai_k, hasegawa_s,
hayasaki}@opt.utsunomiya-u.ac.jp

³Nagoya Institute of
Technology
Aichi, Japan
star@nitech.ac.jp

ABSTRACT

We present a new method of rendering aerial haptic images that uses femtosecond-laser light fields and ultrasonic acoustic fields. In conventional research, a single physical quantity has been used to render aerial haptic images. In contrast, our method combines multiple fields (light and acoustic fields) at the same time. While these fields have no direct interference, combining them provides benefits such as multi-resolution haptic images and a synergistic effect on haptic perception. We conducted user studies with laser haptics and ultrasonic haptics separately and tested their superposition. The results showed that the acoustic field affects the tactile perception of the laser haptics. We explored augmented reality/virtual reality (AR/VR) applications such as providing haptic feedback of the combination of these two methods. We believe that the results of this study contribute to the exploration of laser haptic displays and expand the expression of aerial haptic displays based on other principles.

Author Keywords

Haptic feedback; focused ultrasound; femtosecond laser; laser plasma; aerial interaction.

ACM Classification Keywords

H.5.2. [Information Interfaces and Presentation: User Interfaces];

INTRODUCTION

Aerial haptic feedback is a popular topic in research fields on real-world-oriented interaction, augmented reality (AR), and virtual reality (VR). Various methods such as air jets [1], ultrasound [2], and air vortices [3] have been proposed for this purpose. In the context of visual displays, virtual reality headsets for immersive content and depth cameras for gesture input are being rapidly developed to move from

* Joint first authors.

Permission to make digital or hard copies of all or part of this work for personal or classroom use is granted without fee provided that copies are not made or distributed for profit or commercial advantage and that copies bear this notice and the full citation on the first page. Copyrights for components of this work owned by others than ACM must be honored. Abstracting with credit is permitted. To copy otherwise, or republish, to post on servers or to redistribute to lists, requires prior specific permission and/or a fee. Request permissions from Permissions@acm.org.

CHI'16, May 07-12, 2016, San Jose, CA, USA

© 2016 ACM. ISBN 978-1-4503-3362-7/16/05...\$15.00

DOI: <http://dx.doi.org/10.1145/2858036.2858489>

research laboratories to commercial use by individual consumers. However, a missing and desired function in these immersive technologies is aerial haptic feedback.

Aerial haptic display has several advantages: it projects a force from a distance without physical contact or wearable devices, and it has high programmability. In other words, it can be set and rearranged at an arbitrary position in a 3D space because it does not require physical actuators.

Efforts are continuously being made to render aerial haptic images, and there are now several methods available to do so in a noncontact manner. The fundamental principles of noncontact forces were thoroughly discussed by Brandt [4]. Although he focused on levitation, his work is also applicable to our purpose. There are seven types of noncontact forces: aerodynamic, acoustic, optical, electric, magnetic, radio-frequency, and superconducting technologies. Among them, aerodynamic, acoustic, and optical technologies are potentially available in our daily lives for aerial haptic feedback (Figure 2).

Recently, several studies have focused on the computational design of fields of physical quantities that use graphical and/or holographic approaches, such as acoustic [5] and optical [6] fields. These studies focused on a single physical quantity. In the present study, we focused on methods that combine multiple fields to explore the synergistic effects.

This paper is organized as follows. First, we describe the design of our aerial haptic system (Figure 1). We present the details of the light part (femtosecond laser with a spatial light modulator (SLM) and a galvano mirror) and acoustic part (ultrasonic phased array). Next, we describe the specifications of our system, including the spatial resolution and response time. After that, we report the results of user studies testing the individual and conjugated performances of the light and acoustic fields. Finally, we discuss the applications and user tests. Although we used light and acoustic fields, our results suggest that this approach can also be used to combine multiple other fields.

RELATED WORK

In this section, we review conventional studies on aerial haptic feedback and computational fields. We then point out unresolved issues and clarify the originality of our study.

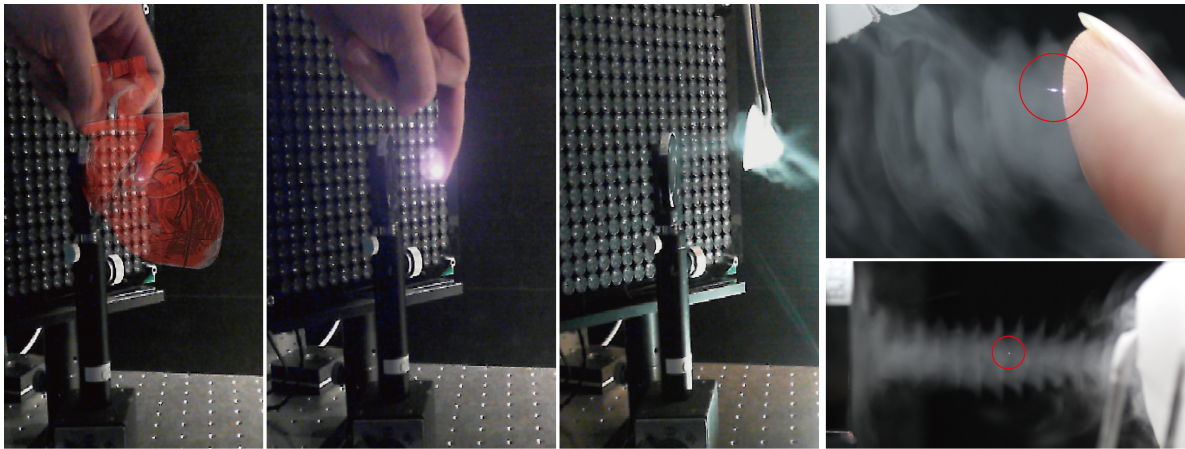


Figure 1. Application images of aerial haptic feedback rendered by laser and ultrasound. (a) An augmented reality image of heart with haptic feedback. (b) Laser plasma. (c) Focused ultrasound visualized by dry ice. (d-e) Close-up.

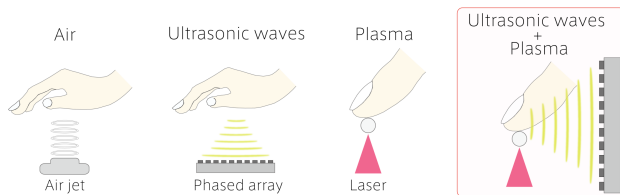


Figure 2: Methods of aerial haptic feedback.

Principle	Study
Aerodynamic	Air jets [Suzuki] Air vortex [Sodhi][Gupta]
Ultrasonic	Radiation pressure [Hoshi][Carter][Inoue]
Optical	Femtosecond laser [Ochiai] Nanosecond laser [Lee] Thermal radiation [Saga]
Magnetic	FingerFlux [Weiss]

This study

Figure 3: A map of related work (aerial haptic feedback).

Aerial Haptic Feedback

Various methods for aerial haptic feedback without physical contact or wearable devices have been proposed. In [1], virtual objects were represented by air jets from an array of nozzles. Air vortices have been used to provide impact in midair [3, 7]. These can be explained as aerodynamic methods. Ultrasonic haptic feedback [2, 8, 9] is highly programmable because of the use of ultrasonic phased arrays. FingerFlux [10] uses magnetic forces by attaching a small magnet to a user’s finger. Light is employed to provide a sensation on the hands when the user is suffering thermal radiation [11]. Nanosecond lasers applied on a skin evoke tactile sensation [12, 13]. Electric, radio-frequency, and superconducting forces have not been applied to aerial haptic feedback so far.

Computational Fields

In some studies, interactions have been designed by computationally controlling fields of physical quantities,

i.e., noncontact forces. The studies on aerial haptic feedback presented above are included in this category. Another purpose is the noncontact control of objects. Poppable Display [14] is a soap film driven by ultrasonic waves to reproduce BRDF. In [15], air jets were used to move objects on a 2D plane. UltraTangibles [16] produces a similar effect by radiation pressure of ultrasound. lapillus bug [17] suspends an object at a fixed height and moves it with an ultrasonic standing wave. Pixie Dust [5] also uses an ultrasonic standing wave to render graphics in midair with levitated particles. ZeroN [18] levitates a magnetic sphere and moves it with an XY stage. [19] and [6] have reported using laser plasma to render aerial images. The latter [6] has also reported that the rendered images can be touched with fingers and they utilized this phenomenon for user interaction. Note that each of these studies controlled the field of a single physical quantity. In other words, they focused on achieving their purpose based on a single principle.

The novelty of our study is to employ two different fields simultaneously and explore not only the superposition but also synergetic effects. This is the first step to developing a new method to combine multiple fields when designing interactions.

Position of This Study

In this study, we aimed to resolve issues with aerial haptic feedback by employing dual fields: light and sound. Our light source was a femtosecond laser with an SLM and galvano mirror, and our sound source was an ultrasonic phased array. As introduced above, touchable laser plasmas have recently been reported while ultrasonic haptic feedback has been closely studied for years. Examining the fundamental characteristics of touchable laser plasma of femtosecond laser is another purpose of this study.

Ultrasonic haptic feedback has a relatively high spatial resolution compared to other aerial haptic feedback methods and is limited by the wavelength (8.5 mm for 40

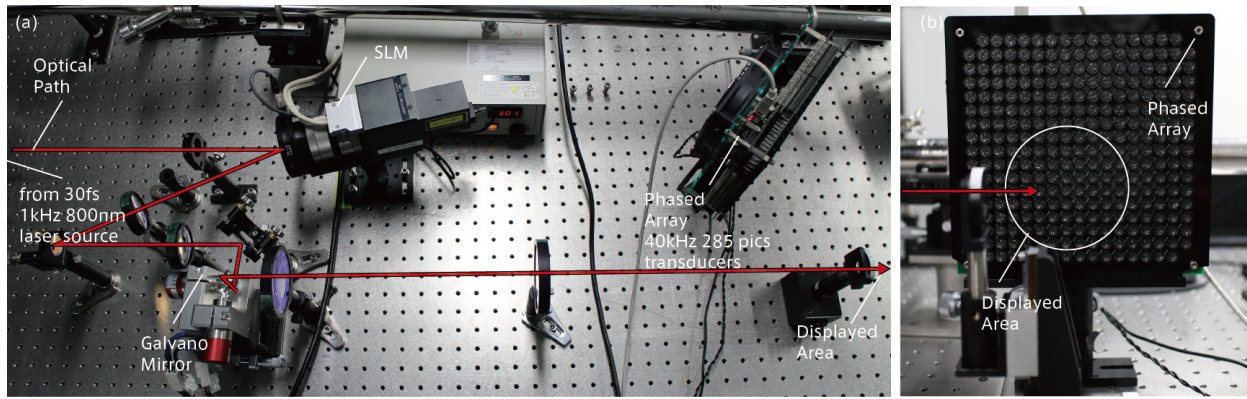


Figure 4: Laser and ultrasonic systems.

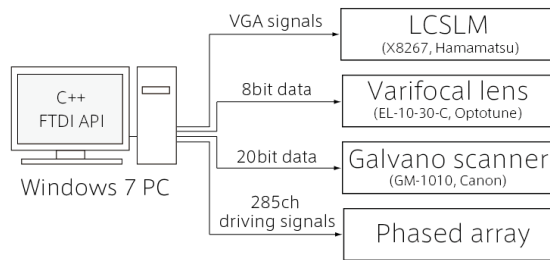


Figure 5: Diagram of control system.

kHz ultrasound). Because of the absorption loss in air, higher-frequency ultrasound (i.e., shorter wavelengths) is not suitable for haptic feedback. Another limitation is the weakness of the stimulation, which is inadequate for reproducing impulses such as the instant of contact. The maximum force generated by an 18×18 array can be as low as 16 mN [2], and a larger array is required to obtain a larger force [20].

We expect that laser plasma may be able to compensate for the shortcomings of ultrasonic haptic feedback. We suppose that these two effects are physically independent of each other. Our motivation is to use these two effects complementarily. They can be applied at the same place and time, and mixed on the skin as elastic wave and/or in the neural system as nerve signals. For example, the laser simulates the encounter of the skin and a virtual object and, after that, the ultrasound produces continuous contact between them.

Combining two fields of different physical quantities would provide not only the superposition effect proposed above but also synergistic effects such as modification of the feeling. Figure 3 describes the focal area of this study.

PRINCIPLES, SYSTEM, AND CONTROL

In this section, we describe the principles of our optic and acoustic systems. First, the optical system, which is a femtosecond laser with an SLM and galvano mirror, is introduced. Next, the acoustic system, which is an ultrasonic phased array, is described. Finally, we describe the control system.

Laser Haptics

The laser haptics is based on evaporation effect of femtosecond laser, which slightly dig the skin surface and generate a shock wave on the skin. This is a non-thermal effect of ultra-short pulse laser (we use 40-fs one in this paper), which is different from thermoelastic effect of nanosecond laser [12, 13]. The application time is limited up to a few seconds to save the skin from damage. The sensation is vivid, little bit painful, and similar to electric stimulation or rough sand paper.

Figure 4 shows an overview of the femtosecond laser, which is followed by an SLM and galvano mirror.

Galvano mirror and lens: Here, we describe our scanning system in detail. We employ galvano mirrors to scan the lateral (X and Y) directions, while a varifocal lens can change its focal point in the beam axial (Z) direction.

SLM: The use of SLMs is one method to render holograms. In general, an SLM has an array of computer-controlled pixels that modulate a laser beam's intensity, phase, or both. A liquid crystal SLM (LCSLM) containing a nematic liquid crystal layer was used in this study. The molecule directions within this layer are controlled by electrodes (i.e., pixels), and the phase of the light ray reflected by each pixel is modulated according to the direction of the liquid crystal molecule. In other words, this device acts as an optical phased array.

The spatial phase control of light enables the focusing position to be controlled along both the lateral (X and Y) and axial (Z) directions. The complex amplitude (CA) of the reconstruction from the computer-generated hologram (CGH) U_r is given by the Fourier transform of the designed CGH pattern U_h :

$$U_r(v_x, v_y) = \iint U_h(x, y) \exp[-i2\pi(xv_x + yv_y)] dx dy$$

$$= a_r(v_x, v_y) \exp[i\phi_r(v_x, v_y)] \quad (1)$$

$$U_h(x, y) = a_h(x, y) \exp[i\phi_h(x, y)] \quad (2)$$

where a_h and φ_h are the amplitude and phase of the hologram plane displayed on the SLM, respectively. In the experiment, a_h is constant because the light irradiation on the CGH is considered to be plane wave with a uniform intensity distribution. φ_h is obtained by using the ORA algorithm, whereas a_r and φ_r are the amplitude and phase of the reconstruction plane, respectively. The spatial intensity distribution of the reconstruction is actually observed as $|U_r|^2 = a_r^2$.

To control the focusing position along the lateral (X and Y) direction, the CGH is designed based on a superposition of CAs of blazed gratings with a variety of azimuth angles. If the reconstruction has N -multiple focusing spots, the CGH includes N -blazed gratings. To control the focusing position along the axial (Z) direction, a phase Fresnel lens pattern $\varphi_p(x, y) = k(x^2 + y^2)/2f$ with a focal length f is simply added to φ_h , where $k = 2\pi/\lambda$ is a wave number. In this case, the spatial resolution of the SLM determines the minimum focal length.

Haptic Images: Haptic images are given by a combination of an SLM image and galvano mirror. Haptic image H_i is the summation of the time series of the focal points, that is,

$$H_i = \sum U_r(v_x, v_y) \times p \times t \quad (3)$$

where U_r represents the laser focal points given by (1), t is time duration, and p is laser intensity.

Ultrasonic Haptics

The ultrasonic haptics is based on acoustic radiation pressure, which is not vibrational and presses the skin surface. This can be applied on the skin for a long time but this is relatively weak (10-20 mN). The sensation is similar to a laminar air flow within a narrow area.

Figure 4 shows an overview of the ultrasonic phased array, which has 285 ultrasonic transducers and controls them individually with adequate time (or phase) delays.

The time delay Δt_{ij} for the (i, j) -th transducer is given by

$$\Delta t_{ij} = \frac{l_{00} - l_{ij}}{c} \quad (4)$$

where l_{00} and l_{ij} are the distances from the focal point to the $(0, 0)$ -th (reference) and (i, j) -th transducers, respectively. c is the speed of sound in air. The focal point can be moved by recalculating and setting the time delays for the next coordinates.

It has been theoretically and experimentally shown that the spatial distribution of ultrasound generated from a rectangular transducer array is nearly shaped like a sinc function [2]. The width of the main lobe w parallel to the side of the rectangular array is written as

$$w = \frac{2\lambda R}{D} \quad (5)$$

where λ is the wavelength, R is the focal length, and D is the length of the side of the rectangular array. This equation

implies that there is a tradeoff between the spatial resolution and array size.

Haptic Images: Haptic images are given by an acoustic phased array system. Haptic image H_i is the summation of the time series of the focal points, that is,

$$H_i = \sum f_p(x, y, z) \times p \times t \quad (6)$$

where f_p is the ultrasonic focal points generated based on (4), p is the acoustic pressure, and t is the time duration.

Control System

Here we describe the pipe line for rendering the haptic image in the air using our system. Figure 5 shows our system diagram. The system is controlled using a Windows PC, with all programs coded in C++. The control system operates the acoustic phased array, SLM, galvano mirror, and varifocal lenses. To monitor the interaction, a USB camera is connected to the system. The phased array, Galvano mirror, and varifocal lenses run along different threads and are synchronized when new draw patterns are input. The user input is captured at 60 Hz, and the SLM is connected to the computer as an external display.

The laser side operation (setting coordinates and controlling the driving mirror, lens, and SLM) is completely performed by the PC. However, the phased array includes an FPGA that receives data, including the coordinate of the focal point and output force, from the PC. On receiving the data, the FPGA calculates adequate time delays for each transducer based on Eqs. (1) and (3), and generates the driving signals. The driving signals are sent to the transducers via the amplifiers. Modifying the time-delay calculation algorithm changes the distribution of the acoustic-potential field. The output force is varied through pulse width modulation (PWM) control of the driving signal.

Hardware Specifications

Light Field: The setup that includes a femtosecond laser light source is described below. This femtosecond laser source (Coherent Co., Ltd.) has a center wavelength of 800 nm, repetition frequency of 1 kHz, and pulse energy in the 1- to 2-mJ range. The Galvano mirror scans the emission dot along the lateral directions (X- and Y-scanning), while the varifocal lens can vary its focal point in the axial direction (Z-scanning). The Fourier CGH is used for parallel optical access [21]. The CGH, designed with an optimal-rotation-angle (ORA) method [22], is displayed on the LCOS-SLM, which has a resolution of 768×768 pixels, pixel size of $20 \times 20 \mu\text{m}^2$, and response time of 100 ms. We employ an Optotune EL-10-30 as the varifocal lens, which is connected via USB serial to a PC. These devices are operated by applications created using C++. The workspace is as large as $2 \times 2 \times 2 \text{ cm}^3$, which is enlarged according to the diameter of the lens.

Acoustic Field: We utilized an ultrasonic phased array (Figure 4) having a resonant frequency of 40 kHz. The

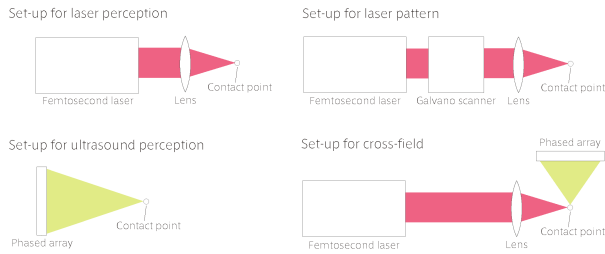


Figure 6: Experimental setup.

position of the focal point is digitally controlled with a resolution of $1/16$ of the wavelength (approximately 0.5 mm for the 40-kHz ultrasound) and can be refreshed at 1 kHz. The 40-kHz phased array consists of 285 transducers (10 mm in diameter, T4010A1, Nippon Ceramic Co., Ltd.) arranged in a $170 \times 170 \text{ mm}^2$ area. The sound pressure at the peak of the focal point is 2585 Pa RMS (measured) when the focal length $R = 200 \text{ mm}$. The size and weight of a single phased array are $19 \times 19 \times 5 \text{ cm}^3$ and 0.6 kg, respectively. It consists of two circuit boards: one is an array board of ultrasonic transducers and the other is a driving board, including an FPGA and push-pull amplifier ICs. These boards are connected to each other with pin connectors. The phased array is controlled by a single PC via USB. The control application is developed in C++ on Windows (Figure 5). The PC sends the data, including the coordinates of the focal point and output force, to the driving board. The driving board receives the data, calculates adequate time delays for each transducer based on Eqs. (1) and (3), and generates the driving signals. The workspace is as large as $30 \times 30 \times 30 \text{ cm}^3$, which is enlarged according to the size of the phased array.

The overlap area of workspace of these laser and ultrasonic haptics is $2 \times 2 \times 2 \text{ cm}^3$, which is limited by the laser haptics. This can be enlarged in future by using a larger lens to enable a larger angle range of the galvano mirror.

USER STUDY AND RESULTS

In this section, we describe the user experiments for evaluating our haptic system. We first describe the evaluation of individual fields, and then describe the synergistic effects between them.

Perceptual Threshold of Laser

We conducted this user study to evaluate the perceptual threshold for shockwaves of laser plasma arisen on skin. Seven subjects participated in this user study (22.5 years old on average, five females and two males). The subjects touched the laser haptic stimulation on their right forefingers. It is difficult to measure the evaporation effect as force (N), and we measure it by the laser output power (W). The laser output power was set at 0.05, 0.10, 0.13, and 0.16 W. The lowest power was limited by the specification and the highest power was determined by the preliminary

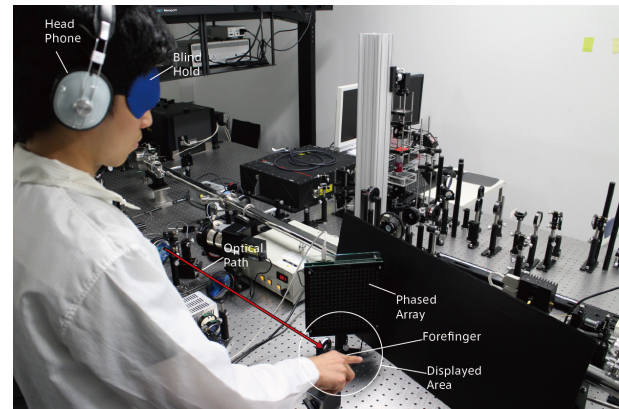


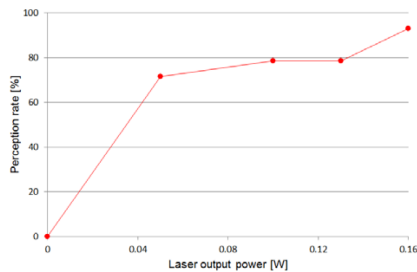
Figure 7: Overview of experimental setup.

tests. Each power condition was applied twice (two trials) and the number of trials was 8 per subject. The order of trials was randomized. In each trial, the subjects touched laser up to 10 times and asked whether they felt something on their forefingers or not. Visual information was shut off by a blindfold and auditory information was blocked off by headphones with white noise (Figure 7).

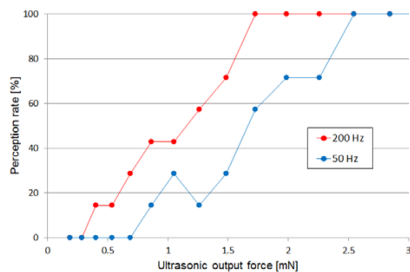
The results are shown in Figure 8 (a). The perception rate is the ratio of the number of trials in which the subjects felt the stimulation to the number of trials of each laser power. The 90% threshold seems to be between 0.03 and 0.04 W. The subjects felt the stimulation confidently (i.e., more than 90%) at 0.16W.

Perceptual Threshold of Ultrasound

We conducted this user study to evaluate the perceptual threshold for acoustic radiation pressure elicited by focused ultrasound. This is the first report on the perceptual threshold of ultrasonic noncontact haptic feedback as far as we know. The subjects were same as the previous section. The direct current output of ultrasound is too weak to be perceivable and hence vibrotactile stimulations (modulated by 200- and 50-Hz rectangular waves) were applied on the forefingers. These modulation frequencies were chosen to well stimulate different channels: PC (Pacian corpuscles) and RA (Meissner corpuscles) [23]. Note that the diameter of ultrasonic focal point (20 mm) is larger than the width of forefinger and the force acting on forefingers is somewhat lower than the output force set by the control system. The output force was set at one of fourteen values around the thresholds that are estimated by the preliminary experiment. Each force condition was applied once (one trial) and the number of trials was 14 per subject. The order of trials was randomized. In each trial, the subjects touched ultrasound freely and asked whether they felt something on their forefingers or not. Visual information was shut off by a blindfold and auditory information was blocked off by headphones with white noise.



(a) Experiment on perceptual threshold of laser.



(b) Experiment on perceptual threshold of ultrasound.

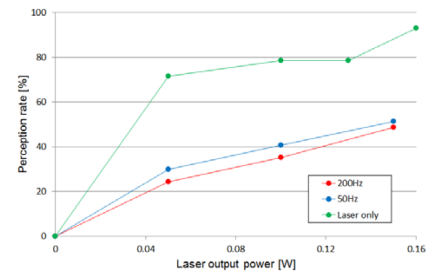
Merged (7 persons)		Answered	
		Dot	Line
Applied	Dot	8	20
	Line	17	11

Inverse (3)		Answered	
		Dot	Line
Applied	Dot	2	10
	Line	11	1

Ambiguous (2)		Answered	
		Dot	Line
Applied	Dot	4	4
	Line	4	4

Bias-toward-line (2)		Answered	
		Dot	Line
Applied	Dot	2	6
	Line	2	6

(c) Experiment on spatial pattern of laser plasma.



(d) Experiment on perceptual threshold of laser accompanied by unperceivable ultrasonic preload.

Figure 8: Experimental results.

The results are shown in Figure 8 (b). The perception rate is the ratio of the number of trials in which the subjects felt the stimulation to the number of trials of each ultrasonic output force. The 50% thresholds for 200- and 50-Hz stimulations seem to be about 1.1 mN and 1.6 mN, respectively. The subjects felt the 200- and 50-Hz stimulations confidently (i.e., 90%) at about 1.6 mN and 2.4 mN, respectively. It is well known in the research field of haptics that the tactile sensitivity is high against about 200-Hz stimulation, and our results agree with this knowledge.

Spatial Patterns of Laser Plasma

We conducted this user study to test the capability to discriminate the spatial patterns rendered with laser plasma. Figure 9 shows examples rendered by repetitive galvanic scan of the laser plasma. In this experiment, two spatial patterns (dot and line) were used. The subjects were same as the previous section. Each pattern was applied four times (four trials) and the number of trials was 8 per subject. The order of trials was randomized. In each trial, the subjects touched laser up to 10 times and asked which pattern they felt on their forefingers. Visual information was shut off by a blindfold and auditory information was blocked off by headphones with white noise.

The results are shown in Figure 8 (c). The merged result indicates that people can discriminate the two patterns but tend to answer inversely. The correct rate would become better once they recognize the patterns. It is to be noted that some of the subjects could discriminate the two patterns very well (“inverse” group) however the others could not at all. Furthermore, there were two types of tendency: one is an “ambiguous” group and the other is a “bias-to-line” group. There is a room for further investigation.

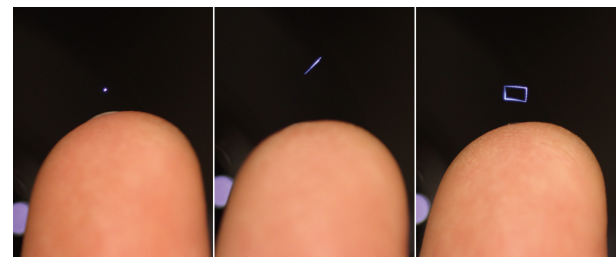


Figure 9: Spatial patterns rendered with laser plasma (dot, line, and box).

Perceptual Threshold of Cross-Field

We conducted this user study to evaluate the perceptual threshold for shockwaves of laser plasma under the preload of ultrasonic vibrotactile stimulation that is weaker than the perceptual threshold. There are two possible effects of ultrasound on the laser haptics. One is a masking effect that increases the perceptual threshold for laser plasma, and the other is a stochastic effect that decreases it.

Nine subjects participated in this user study (21.6 years old on average, four females and five males). The subjects touched the laser haptic stimulation on their right forefingers. The laser power was set at 0.05, 0.10, and 0.15W. The modulation frequency of ultrasound was 200 Hz and 50 Hz to stimulate PC and RA channels, respectively. Each power and frequency condition was applied four times (four trials) and the number of trials was 24 per subject. The order of trials was randomized. In each trial, the subjects touched laser up to 10 times and asked whether they felt something on their forefinger or not. The ultrasonic stimulation was tuned to be just under the perceivable force for each frequency and subject. Visual information was shut off by a blindfold and auditory

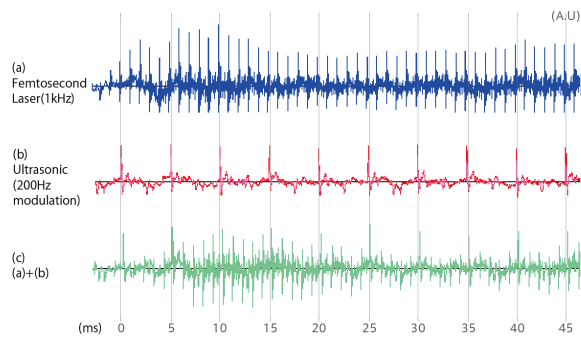


Figure 10: Audible sound radiated from contact point.

information was blocked off by headphones with white noise. Figure 10 shows the audible sound from the laser and ultrasonic haptic stimulation.

The results are shown in Figure 8 (d), where “Laser only” is identical to Figure 8 (a). It is interesting that the ultrasound, weaker than the perceptual threshold, affects the perception of laser shock wave. The 50% perceptual threshold for the laser haptics with unperceivable ultrasonic preload (red and blue lines in Figure 8 (d)) is around 0.15W, which is nearly 5 times larger than that of “Laser only” (green line).

The results support the masking effect. This means that the ultrasonic preload makes the laser haptics less surprising and less painful. The mechanism of this masking effect is included in future work.

APPLICATION

In this section, we discuss applications of the proposed method. First, we describe the characteristics of the method. We then outline the possible applications: haptic interactions based on the cross-field aerial haptic feedback.

Application Domain

The characteristics of our cross-field aerial haptic method include

1. The ultrasonic phased array can produce haptic images roughly (spatial resolution is 16 mm, twice of the wavelength) however it can cover large areas (around 30 cm) and radiation pressure is adequately strong (16 mN).
2. The femtosecond laser system can produce haptic images precisely (spatial resolution 1 μm) however it can cover only small areas (up to 2 cm).
3. The ultrasound represses the human sensitivity to the laser plasma as found in the experiment on the perceptual threshold of cross-field.

In this paper, we employ the acoustic field for rough haptic images and awareness for laser haptic. On the other hand, we employ the light field for detailed haptic images. Then, we implemented haptic images for AR/VR applications which express an object surface (rough) by ultrasound and inner structure and/or indication (detailed) by laser,

awareness by ultrasound and Braille alphabets by laser, and extension of ultrasonic haptics by laser.

Multi-resolution haptics for VR

In this application, roughly covered haptic image is generated by ultrasonic acoustic field. Adding to the acoustic field, high resolution haptic image by plasma is used for precise expression for pointing or inner structure of target 3D models. Figure 6 shows setup of our system. AR marker used for matching coordinates between camera view and 3D object. When participants put their fingers into the models, firstly they feel outer haptic image which corresponding to virtual models in AR. After that, participants feel the laser plasma haptics in the floating models.

This plasma works as an indicator to a precise point (ex., a tumor in organs, pointer of 3D haptic map, etc.). This application extends conventional ultrasonic haptics in the resolution and the variety of tactile feedback patterns.

Aerial Braille Alphabet

In this application we utilize our system’s advantage for aerial haptic image. Conventional braille alphabet display is made of pin actuator arrays or other contact type display. In conventional ultrasonic or air jet haptic display cannot create precise and high resolution haptic image. Our display can express tiny haptic image in the air and also we can generate arbitrary position in air. This is useful characteristic for braille alphabet display. It will change the interaction with Braille Alphabet from “touch” to “come”. To indicate the area for haptic image we utilize acoustic field. Then user find the haptic image area and insert their finger to it, they can feel plasma haptic feedback from it.

DISCUSSION

In this section, we discuss the scalability, perception, and safety based on the user study and application design.

Scalability

The force of the ultrasound radiated from a single phased array increases according to the number of transducers. More transducers enable us to generate more powerful acoustic radiation pressure. Increasing the number of transducers results in other benefits. One such benefit is a larger workspace keeping the size of the focal point. Another is smaller dispersion of the phase delay characteristics of transducers, which leads to more accurate generation and control of the acoustic field.

The pulse duration is an important factor in the laser haptics. Shorter pulse duration gives higher peak power with the same time-averaged power. Shorter pulse duration also gives higher repetition frequency of laser pulses.

Resolution and Perception

From the result of our study, acoustic radiation pressure can mask the sensation of laser haptic feedback. In this study we tested both light and acoustic fields. We have explored around the technologies in spatial factors that we investigated the 3D shape and 3D point of cross-field haptic

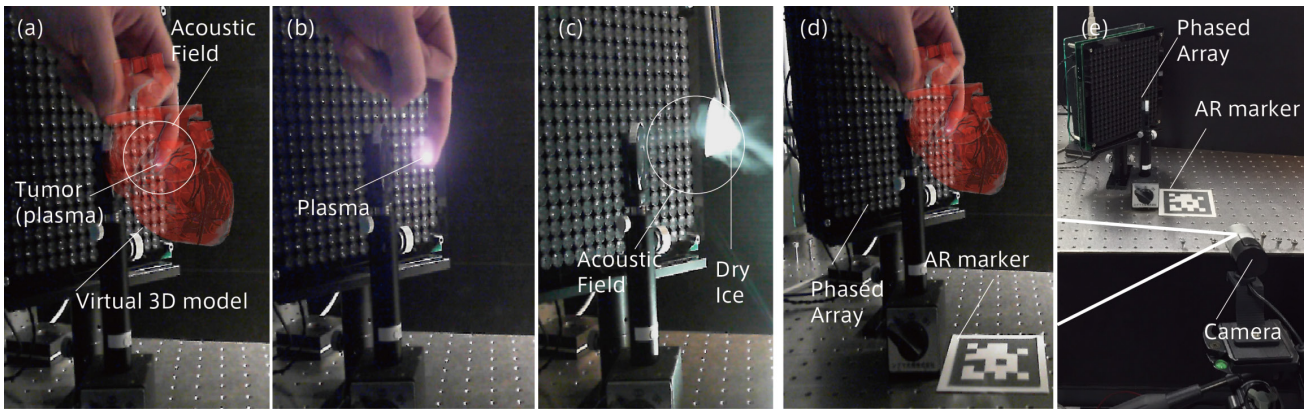


Figure 11: AR application of tumor in heart.

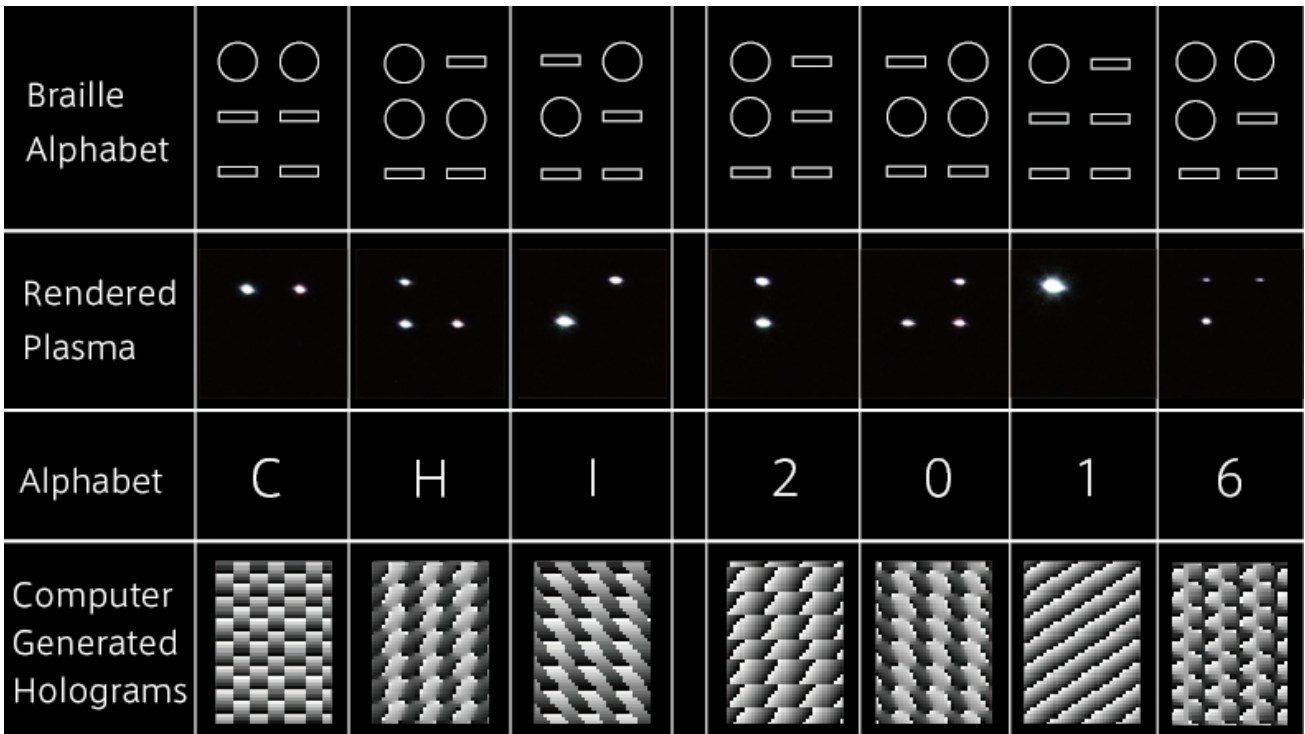


Figure 12: Application of Braille dots.

images. We have not explored the time domain factors. This will be the next topic of field-driven aerial haptic research.

Risk of Laser

Damage to skin by femtosecond lasers was experimented using porcine skin in [24]. It was reported that the lesions by the 44-fs pulse laser whose pulse energy is less than 21 mJ disappeared at 24 hours after exposure. The maximum pulse energy of our current system is up to 2 mJ, and hence we expect that the skin damage by our laser haptics is negligible.

Damage to retina should be concerned when we apply our technologies to daily lives. The laser system should be carefully designed not to shoot users' eyes directly. We employed infrared laser (800nm in wavelength) and a filter

that cuts off this wavelength is an efficient way to ensure retina.

CONCLUSION

In this paper, we present a new method of rendering aerial haptic images using femtosecond-lasers light fields and ultrasonic acoustic fields. Compared to conventional methods, our method offers the advantage of simultaneously combining multiple fields (light and acoustic fields).

We implemented our system using an ultrasonic phased array and laser induced plasma. While these fields have no direct interference, their combination offers benefits such as multi-resolution haptic images and synergistic effects on haptic perception. Our results show that the acoustic field affects tactile perception of the laser haptics. The findings

are as follows; laser tactile sensation is repressed in an acoustic field; some users can differentiate spatial patterns rendered with laser plasma; users can detect the 3D position of the laser stimulation better than the ultrasonic stimulation. Then, we explored AR/VR applications in fields such as medicine to provide haptic feedback of the shape of an organ using acoustic radiation pressure and the especially indicated position using laser-excited shock waves. We built four applications to combine these two physical quantities.

We believe that this study contributes to the exploration of haptic displays based on femtosecond lasers, which have not been well investigated, and to the expansion of the expression of aerial haptic displays based on other principles.

REFERENCES

1. Yuriko Suzuki and Minoru Kobayashi. 2005. Air jet driven force feedback in virtual reality. *Computer Graphics and Applications*, IEEE 25, 1 (Jan), 44-47. DOI: <http://dx.doi.org/10.1109/MCG.2005.1>
2. Takayuki Hoshi, Masafumi Takahashi, Takayuki Iwamoto, and Hiroyuki Shinoda. 2010. Noncontact tactile display based on radiation pressure of airborne ultrasound. *IEEE Transactions on Haptics* 3, 3, 155-165. DOI: <http://dx.doi.org/10.1109/TOH.2010.4>
3. Rajinder Sodhi, Ivan Poupyrev, Matthew Glisson, and Ali Israr. 2013. Aireal: Interactive tactile experiences in free air. *ACM Trans. Graph.* 32, 4 (July), 134:1-134:10. DOI: <http://dx.doi.org/10.1145/2461912.2462007>
4. E.H. Brandt. 1989. Levitation in physics. *Science* 243, 4889, 349-355. DOI: <http://dx.doi.org/10.1126/science.243.4889.349>
5. Yoichi Ochiai, Takayuki Hoshi, and Jun Rekimoto. 2014. Pixie dust: Graphics generated by levitated and animated objects in computational acoustic-potential field. *ACM Trans. Graph.* 33, 4 (July), 85:1-85:13. DOI: <http://dx.doi.org/10.1145/2601097.2601118>
6. Yoichi Ochiai, Kota Kumagai, Takayuki Hoshi, Jun Rekimoto, Satoshi Hasegawa, and Yoshio Hayasaki. 2015. Fairy lights in femtoseconds: Aerial and volumetric graphics rendered by focused femtosecond laser combined with computational holographic fields. In *ACM SIGGRAPH 2015 Emerging Technologies*, ACM, New York, NY, USA, SIGGRAPH '15. DOI: <http://dx.doi.org/10.1145/2782782.2792492>
7. Sidhant Gupta, Dan Morris, Shwetak N. Patel, and Desney Tan. 2013. AirWave: Non-contact haptic feedback using air vortex rings. In *Proceedings of the 2013 ACM International Joint Conference on Pervasive and Ubiquitous Computing*, ACM, New York, NY, USA, UbiComp '13, 419-428. DOI: <http://dx.doi.org/10.1145/2493432.2493463>
8. Tom Carter, Sue Ann Seah, Benjamin Long, Bruce Drinkwater, and Sriram Subramanian. 2013. Ultrahaptics: Multi-point mid-air haptic feedback for touch surfaces. In *Proceedings of the 26th Annual ACM Symposium on User Interface Software and Technology*, ACM, New York, NY, USA, UIST '13, 505-514. DOI: <http://dx.doi.org/10.1145/2501988.2502018>
9. Seki Inoue, Koseki J. Kobayashi-Kirschvink, Yasuaki Monnai, Keisuke Hasegawa, Yasutoshi Makino, Hiroyuki Shinoda. 2014. HORN: The hapt-optic reconstruction. In *ACM SIGGRAPH 2014 Emerging Technologies*, ACM, New York, NY, USA, SIGGRAPH '14, 11:1. DOI: <http://dx.doi.org/10.1145/2614066.2614092>
10. Malte Weiss, Chat Wacharamanatham, Simon Voelker, and Jan Borchers. 2011. Fingerflux: Near-surface haptic feedback on tabletops. In *Proceedings of the 24th Annual ACM Symposium on User Interface Software and Technology*, ACM, New York, NY, USA, UIST '11, 615-620. DOI: <http://dx.doi.org/10.1145/2047196.2047277>
11. Satoshi Saga. 2014. HeatHapt: Thermal-radiation-based haptic display. *AsiaHaptics 2014*.
12. Jae-Hoon Jun, Jong-Rak Park, Sung-Phil Kim, Young Min Bae, Jang-Yeon Park, Hyung-Sik Kim, Seungmoon Choi, Sung Jun Jung, Seung Hwa Park, Dong-Il Yeom, Gu-In Jung, Ji-Sun Kim and Soon-Cheol Chung. 2015. Laser-induced thermoelastic effects can evoke tactile sensations. *Scientific Reports* 5, 11016. DOI: <http://dx.doi.org/10.1038/srep11016>
13. Hojin Lee, Ji-Sun Kim, Seungmoon Choi, Jae-Hoon Jun, Jong-Rak Park, A-Hee Kim, Han-Byeol Oh, Hyung-Sik Kim, and Soon-Cheol Chung. 2015. Mid-air tactile stimulation using laser-induced thermoelastic effects: The first study for indirect radiation. In *World Haptics Conference (WHC)*, 2015, 374-380. DOI: <http://dx.doi.org/10.1109/WHC.2015.7177741>
14. Yoichi Ochiai, Takayuki Hoshi, Alexis Oyama, and Jun Rekimoto. 2013. Poppable display: A display that enables popping, breaking, and tearing interactions with people. In *Consumer Electronics (GCCE)*, 2013 IEEE 2nd Global Conference on, 124-128. DOI: <http://dx.doi.org/10.1109/GCCE.2013.6664771>
15. Satoshi Iwaki, Hiroshi Morimasa, Toshiro Noritsugu, and Minoru Kobayashi. 2011. Contactless manipulation of an object on a plane surface using multiple air jets. In *ICRA*, IEEE, 3257-3262. DOI: <http://dx.doi.org/10.1109/ICRA.2011.5979879>
16. Mark Marshall, Thomas Carter, Jason Alexander, and Sriram Subramanian. 2012. Ultra-tangibles: Creating movable tangible objects on interactive tables. In *Proceedings of the SIGCHI Conference on Human Factors in Computing Systems*, ACM, New York, NY,

- USA, CHI '12, 2185-2188. DOI: <http://dx.doi.org/10.1145/2207676.2208370>
17. Michinari Kono, Yasuaki Kakehi, and Takayuki Hoshi, 2013. lapillus bug. SIGGRAPH Asia 2013 Art Gallery.
 18. Jinha Lee, Rehmi Post, and Hiroshi Ishii. 2011. ZeroN: Mid-air tangible interaction enabled by computer controlled magnetic levitation. In Proceedings of the 24th Annual ACM Symposium on User Interface Software and Technology, ACM, New York, NY, USA, UIST '11, 327-336. DOI: <http://dx.doi.org/10.1145/2047196.2047239>
 19. Hidei Kimura, Taro Uchiyama, and Hiroyuki Yoshikawa. 2006. Laser produced 3D display in the air. In ACM SIGGRAPH 2006 Emerging Technologies, ACM, New York, NY, USA, SIGGRAPH '06. DOI: <http://dx.doi.org/10.1145/1179133.1179154>
 20. Keisuke Hasegawa and Hiroyuki Shinoda. 2013. Aerial display of vibrotactile sensation with high spatial-temporal resolution using large-aperture airborne ultrasound phased array. In World Haptics Conference (WHC), 2013, 31-36. DOI: <http://dx.doi.org/10.1109/WHC.2013.6548380>
 21. Yoshio Hayasaki, Takashi Sugimoto, Akihiro Takita, and Nobuo Nishida. 2005. Variable holographic femtosecond laser processing by use of a spatial light modulator. Appl. Phys. Lett. 87, 031101. DOI: <http://dx.doi.org/10.1063/1.1992668>
 22. Jörgen Bengtsson. 1994. Kinoform design with an optimal-rotationangle method. Appl. Opt. 33, 29 (Oct), 6879-6884. DOI: <http://dx.doi.org/10.1364/AO.33.006879>
 23. S.J. Bolanowski, Jr., G.A. Gescheider, R.T. Verrillo, and C.M. Checkosky. 1968. Four channels mediate the mechanical aspects of touch. The Journal of the Acoustical Society of America. 84, 5, 1680-1694.
 24. Clarence P. Cain, William P. Roach, David J. Stolarski, Gary D. Noojin, Semih S. Kumru, Kevin L. Stockton, Justin J. Zohner, and Benjamin A. Rockwell. 2007. Infrared laser damage thresholds for skin at wavelengths from 0.810 to 1.54 microns for femto-to-microsecond pulse durations. In Proc. SPIE. Vol. 6435. 64350W. DOI: <http://dx.doi.org/10.1117/12.715199>